CONF-760910--1

MASTER

EFFECTS OF MICROSTRUCTURE ON ULTRASONIC EXAMINATION OF STAINLESS STEEL

D. S. Kupperman and K. J. Reimann

Specialist Meeting on Ultrasonic Inspection
of Reactor Components
Risley, England
September 27-29, 1976

UNIC-AUA-USERDA

ARGONNE NATIONAL LABORATORY, ARGONNE, ILLINOIS

operated under contract W-31-109-Eng-38 for the
U. S. ENERGY RESEARCH AND DEVELOPMENT ADMINISTRATION

EFFECTS OF MICROSTRUCTURE ON ULTRASONIC EXAMINATION OF STAINLESS STEEL*

by

D. S. Kupperman and K. J. Reimann

Argonne National Laboratory
Materials Science Division
Argonne, Illinois 60439

ABSTRACT

Ultrasonic inspection of cast stainless steel components or stainless steel welds is difficult, and the results obtained are hard to interpret. The present study describes the effects of stainless steel microstructure on ultrasonic test results. Welded coupons, 2.5 and 5.0 cm thick, were fabricated from Type 304 stainless steel, with Type 308 stainless steel as the weld material. Metallography of the base material shows grain sizes of 15 and 80 μm, and dendrites aligned from the top to the bottom surface in cast material. X-ray diffraction and ultrasonic velocity measurements indicate a random crystal orientation in the base material, but the cast sample had aligned dendrites. The weld material exhibits a dendritic structure with a preferred <100> direction perpendicular to the weld pass. Spectral analysis of ultrasonic broad-band signals through the base materials shows drastic attenuation of higher frequencies with increasing grain size (Rayleigh scattering). Annealing and recrystallization increases the ultrasonic attenuation and produces carbide precipitation at grain boundaries. The microstructural differences of the base metal, heat-affected zone, and weld metal affect the amplitude of ultrasonic reflections from artificial flaws in these zones. Data obtained from two samples of different grain sizes indicate that grain size has little effect when a 1-MHz transducer is used. When going from a 15 to an 80-μm crystalline structure, a 5-MHz unit suffers a 30-dB attenuation in the detection of a 1.2 mm deep notch. The anisotropy of the dendritic structure in stainless steel renewed the interest in the effect of shear-wave polarization. In the <110> crystallographic orientation of stainless steel, two modes of shear waves can be generated, which have velocities differing by a factor of two. This effect may be helpful in "tuning" of shear waves by polarization to obtain better penetration in large grain materials such as welds.

---

*Work supported by the U. S. Energy Research and Development Administration.

INTRODUCTION

Ultrasonic inspection of cast stainless steel components or stainless steel welds is difficult, and the results obtained are not easily interpreted. In many instances, however, only ultrasonic techniques are applicable, especially when periodic volumetric inspection in a radioactive environment may be required. Spurious signals, which cannot be correlated with component geometry or actual flaws, contribute to the difficulties when interpreting the results. These spurious signals can often be related to the microstructure of stainless steel welds. In the present investigation, some of the effects of microstructure on the behavior of ultrasonic waves in stainless steel will be evaluated.

In previous investigations, it has been shown, for example, that shear waves are severely attenuated in cast stainless steel,[1,2] thus inhibiting the use of conventional shear-wave testing. Furthermore, local refraction of longitudinal beams has made reflector location somewhat difficult, although short pulses and beam focusing can improve ultrasonic testing in some cases.[1,3] Both observations are related to the microstructure of the materials. Studies have also been made on the relationship of ultrasonic attenuation and grain size in stainless steel.[4]

In the present work, the capability of detecting artificial flaws in stainless steel specimens with different grain sizes is considered. Also, the effects of variations in microstructure on velocity of sound, attenuation, and flaw-detection capabilities for both transverse and longitudinal waves are examined.

EXPERIMENTAL PROCEDURES

Sets of welded Type 304 stainless steel plates were fabricated and cut into samples that were 75-mm wide, 150-300 mm long, and 12.5-50 mm thick.

The first set of specimens consisted of welded Type 304 stainless steel plates with different grain sizes and varying percentages of delta-ferrite in the weld metal. They were fabricated from hot-rolled 25-mm-thick plate and laboratory heat treated at various temperatures to obtain grain-size differences. Two weld metals were used, and the edge was prepared for welding in a double V-shape with a 60° included angle. Electric-discharge-machined (EDM) notches were placed in the weld metal and the heat-affected-zone (HAZ) for ultrasonic measurements (Fig. 1).

The second set of welded specimens varied in thickness between 12.5 and 50 mm and was also fabricated from hot-rolled plates. The samples exhibited a uniform, small grain-size microstructure. Some specimens were subsequently heat treated to evaluate the effects of sensitization on ultrasonic wave propagation.

The third set of 25-mm-thick specimens was obtained from a vacuum melted, vacuum chill-cast ingot of Fe-20 Ni-20 Cr austenitic stainless

steel. These samples had a dendritic microstructure with the dendrites extending through the entire plate thickness. The plates were joined with a butt weld, using Type 308 stainless steel as weld material. The total included angle of the weld was 77°. The characteristics of the samples are summarized in Table 1.

Table 1. Description of Welded Stainless Steel Plates

Plate No.	Base Metal	Weld Metal	Heat Treatment	Base Metal Grain Size	Comments
Group A - Different Grain Sizes					
1A	304 SS	316 SS	1/2 h at 954°C	ASTM 9, 15 μm	Ferrite free, minimum amount of microfissuring in weld metal
2A	304 SS	308 SS	1/2 h at 954°C	ASTM 9, 15 μm	Some δ ferrite
3A	304 SS	316 SS	1/2 h at 1121°C	ASTM 4, 80 μm	Ferrite free, minimum amount of microfissuring in weld metal
4A	304 SS	308 SS	1/2 h at 1121°C	ASTM 4, 80 μm	Some δ ferrite
Group B - Sensitized vs Nonsensitized					
1B	304 SS	308 SS	none	ASTM 6, 40 μm	No carbide precipitation in base metal
2B	304 SS	308 SS	1 h at 500°C furnace cooled	ASTM 6, 40 μm	Carbide precipitation at grain boundaries in base metal
Group C - Cast Stainless Steel					
1C	20Ni-20Cr	308 SS	None	Dendrites 25 mm long	8% delta ferrite in weld metal

The specimens were machined flat on all surfaces after the welding operation to facilitate measurements. Grain-size measurements were obtained from metallographic inspections after the entire sample or cut out coupons were etched in glyceregia. Data concerning preferred crystal orientation in the cast specimen were acquired by X-ray diffraction measurements using a General Electric X-ray diffractometer. The diffractometer with a 60-mm^2 beam from a CuK_α tube scanned the sample at a rate of 2°/min.

Ultrasonic measurements were performed with a variety of narrow- and wideband, shear- and longitudinal-wave transducers in the 1-10 MHz, frequency range. An Aerotech UTA Transducer Analyzer or a Branson 303B Pulser Receiver supplied the ultrasonic energy, and a Hewlett-Packard spectrum analyzer and/or Tektronix 7613 oscilloscope provided the data displays. Various ultrasonic measurements were taken, and the results were compared with the microstructure of the specimens to establish a correlation.

RESULTS AND DISCUSSION

1. Metallography

The difference in grain size of the base metal for plates 2A and 4A can be observed in Figs. 2 and 3. The average grain size in Fig. 2 is ~15 μm, whereas the grain size in Fig. 3 has increased to 80 μm. Essentially no difference was noted in the appearance of the weld metal. The weld metal exhibits dendritic structures, emanating at the fusion line, that are aligned more or less perpendicular to the fusion line.

Photomicrographs of coupons from plates 1B and 2B, (before and after sensitization) showed typical increases in carbide precipitation at the grain boundaries. No significant change in grain size was observed as a result of the heat treatment.

Long columnar grains, formed parallel to the original plate solidification direction, are evident through the macro-etched thickness of plate 1C (Fig. 4). The grain cross-sectional areas increase through the thickness of the plate, an effect that would be expected in cast pipe. This occurs because the high nucleation rate present in the first metal to solidify against the cold mold wall produces a fine microstructure. The subsequent slower solidification, radially inward from the outside mold wall, is controlled by heat transfer through the solidified layer of the pipe and produces a coarser structure.

2. X-ray Diffraction Measurements

The relative intensities of X-ray Bragg peaks for various crystallographic planes were recorded at different locations on the base metals of the cast sample.

The results of X-ray diffractometer scanning at two locations in the plate show a high proportion of (200) intensity relative to that normally present in a polycrystalline specimen. An indication of preferred growth in the <100> solidification direction is found in face-centered-cubic (fcc) materials. It was not possible to obtain X-ray diffraction results that indicated preferred grain growth for a beam directed perpendicular to the solidification direction because the grains were too large.

3. Ultrasonic Velocity Measurements

A velocity profile, representative of specimens in groups A and B, is shown in Fig. 5. A variation in sound velocity of ~4% can be observed for the base and weld metals. Figure 6 shows a similar profile for the group C cast stainless steel. The highest (<111>) and lowest (<100>) single-crystal longitudinal velocities of sound in austenitic stainless steel are also indicated in the Fig. 5. The velocity measured parallel to the dendrite long axis ($v_{\parallel}$) is close to the single- crystal velocity in the <100> direction. This is in agreement with the X-ray diffraction results, which indicate a preferred <100> texture in this direction. The velocity perpendicular to the dendrites, $v_{\perp}$, approaches the polycrystalline longitudinal velocity which indicates little preferred orientation along the ultrasonic beam. As the ultrasonic beam traverses many grain boundaries and dendrites of various crystallographic orientations while moving perpendicular to the solidification direction, its velocity approaches the polycrystalline velocity, which is in agreement with the present data.

The change in longitudinal velocity at different positions along the sample length is reproducible and indicates the variability of grain orientation with respect to position in the specimen. This points out the sensitivity of velocity measurement as an index of crystallographic texture. In large-grain samples such as this one, the velocity of sound method is superior to the X-ray technique for texture determination.

In the weldment, a slightly lower velocity of sound was found in the Y- direction (parallel to the dendrites), which suggests a <100> preferred orientation for the Y-direction over the Z-direction in the weld metal. A comparison of Figs. 5 and 6 indicates that some preferred orientation of crystals in the weld material exists, but it is not as pronounced as in the dendritic structure of the cast base material. The crystal orientation of hot-rolled plate, on the other hand, is random. Therefore, these types of velocity measurements could be used as indicators of orientation in the crystalline structure of metals. A difference in acoustic velocity between the base metal and the weld metal will cause a change in the direction of an ultrasonic beam; the beam does not impinge perpendicular to the interface. As a result, the reflectors can be inaccurately located. Moreover, differences in acoustic impedance due to the change in sound velocity could result in spurious ultrasonic echoes.

4. Spectral Analysis

Ultrasonic spectroscopy yields useful information about the properties of the materials under investigation.[7,8] A significant difference in acoustic properties exists among the samples of group A, as can be seen in the "A" scan as well as the frequency spectrum in Figs. 7 and 8. Severe attenuation of the longitudinal waves is observed at frequencies above 3 MHz in specimens with the larger grain structure, whereas strong

signals, even beyond 10 MHz, are present in the sample with the smaller grain-size. The shear-wave spectra are similar to the longitudinal wave spectra and reflect the change in wave length associated with the switch from longitudinal to shear waves.

Figure 9 shows the frequency spectra from specimens 1B obtained with a broadband, longitudinal wave transducer. At higher frequencies (15 MHz), the drop in attenuation is significantly greater than at lower frequencies. The figure indicates that, in the as-welded condition, the sound wave is more attenuated in weld metal than in the base metal. Moreover, higher frequencies are more strongly affected in the direction perpendicular to the dendrites.

Similar results were obtained with the cast samples of group C, as is evident in Fig. 10. The spectra for carbon steel and plexiglass, taken with the same transducer, are shown for comparison. A rather large attenuation at all frequencies in the weld metal is noted (Figs. 9 and 10) when the required acoustic energies are compared.

The results of spectral analyses indicate that, for weld inspection in stainless steel, frequencies below 2 MHz may be more effective. The variation in attenuation between weld metal and base metal will introduce large inaccuracies when determining defect sizes in the weld metal.

5. Ultrasonic Attenuation

Samples of group B showed a slight decrease in attenuation at higher frequencies after sensitization. To determine accurately the magnitude of the effect, which might influence flaw detectability in the HAZ, for example, echo-decay curves were obtained for as-welded and sensitized conditions using 2.25 and 15 MHz transducers. Figure 11 shows the echo amplitude at two ultrasonic frequencies before and after sensitization. The curves represent the average data acquired at 1 cm from each side of the weld centerline. Data obtained at other positions did not differ considerably from these results. The cause of the change in attenuation observed is not apparent. A possible explanation might be a reduction in ultrasonic reflection at the grain boundaries due to the presence of carbide precipitates.

The dendritic structure of specimen 1C and the weld metals of all specimens exhibited behavior typical of anisotropic material. The longitudinal waves in specimen 1C were less severely attenuated than the shear waves.

These results suggest that sensitization will not affect ultrasonic testing detrimentally, and longitudinal waves may be more appropriate to penetrate larger grain-size stainless steel components.

6. Flaw-detection Capability

Although shear waves present problems when applied to inspection of stainless steel welds, they are widely used for this purpose. To assess how the defect-detection capabilities vary with microstructure changes, the specimens of group A were examined using a variety of transducer frequencies and beam angles. Commercially available narrowbandwidth shear-wave transducers and instrumentation were used for this task. The EDM notches, as shown in Fig. 1, have been placed in the weld metal and near the weld fusion line. Table 2 summarizes the data obtained from these measurements in 25-mm-thick samples.

Table 2. Ultrasonic Signal Amplitude

Transducer[a]		Relative Ultrasonic Signal Amplitude from Notch					
		Welded Plates with Small-grain Base Metal			Welded Plates with Large-grain Base Metal		
Frequency, MHz	Beam Angle, deg	Base Metal	Weld Metal (308)	Weld Metal (316)	Base Metal	Weld Metal (308)	Weld Metal (316)
5	45	9	0.6	1	0.2	-	0.1
5	60	1	-	-	-	-	-
2.25	45	50	10	9	30	8	7
2.25	60	4	4	3	3	3	3
1	45	25	12	12	25	16	12
1	60	4	3	3	4	3	3

[a]13-mm diameter

As anticipated from frequency analysis, signals from 5 MHz probes vary significantly more with grain size than the 2.25- and 1-MHz transducers. A difference of 25 dB in signal amplitude, was obtained at 5 MHz for the two grain sizes, whereas no difference was observed at 1 MHz. Notches in the weld metal were more difficult to detect, and the amplitude was much smaller. Because sensitization does not appreciably affect the results of ultrasonic testing, no measurements were performed on specimens of group B.

In the cast stainless steel specimen of group C, small artificial flaws were introduced to evaluate flaw-detection capability. Two small holes were drilled in the specimen; a 1.6-mm-dia hole, 12.5 mm long was placed in the side of the base metal about 75 mm from the weld and 4 mm from the bottom of the sample, and the other 0.8-mm-dia hole was drilled in the center of the weld metal. Two notches 1.5 mm deep and 6.3 mm long were placed (a) in the weld metal and (b) in the base metal 6.3 mm from the fusion line.

As could be anticipated, these flaws were undetectable with shear waves; however, some success was achieved with longitudinal waves. In the latter case, a 2.25-MHz longitudinal wave was coupled through a steel wedge to the specimen in such a way that 45° longitudinal waves were generated. The reflections from the holes were larger than other signals by a ratio of 2:1 for the 1.6 mm hole in the base metal and 4:1 for the 0.8 mm hole in the weld metal. The 1.5 mm deep notch in the weld metal could not be detected. The base-metal notch was detectable but with considerable difficulty. The measurements were performed on 25-mm-thick cast stainless steel samples. The results indicate that flaw detection capability in stainless steel may decrease with an increase in grain size. The shear waves can be used most effectively for inspection of fine grain stainless steel. Stainless steel welds, which exhibit some dendritic microstructure, are inspected with lower frequency shear waves or possibly longitudinal waves. The higher attenuation in the weld metal, compared with small grain-size base metal, should be taken into account when attempting to size flaws or establishing distance-amplitude-correction (DAC) curves.

7. Shear-wave Polarization

In single crystals and polycrystalline materials with preferred orientation, attenuation and frequency spectra of shear waves can be altered (because of the anisotropy) when the polarization of the waves is varied. The effects of changes in the polarization of shear waves in stainless steel were explored to determine whether these changes can provide more information about ultrasonic reflectors. Shear waves were propagated in a direction parallel to the weld-pass direction in the 300 x 25 x 25 mm stainless steel weld sample shown in Fig. 12. Two 5-MHz, 13-mm (1/2-in.)-dia shear-wave transducers in a through-transmission mode were employed to record the frequency spectra while the polarization angle θ was varied. The <100> preferred orientation of this weld was in the Z-direction. The shear wave was polarized along the <100> direction when $\theta = 0°$.

Figure 13 indicates the difference in the radio-frequency (rf) "A" scan and frequency spectra for two shear waves traveling in the Y-direction, as shown in Fig. 12. The shear wave polarized in the <100> preferred direction ($\theta = 0°$) of the weld has less attenuation at higher frequencies than the shear wave polarized in the X-direction ($\theta = 90°$).

The peak-to-peak rf signals for the two polarizations also differ by 3 dB; the wave polarized in the <100> preferred directions ($\theta = 0°$) has the least attenuation. A difference of ~25% in the velocity of sound also exists, as indicated by the different transit times of the received pulse. Data obtained from Type 304 stainless steel base metal showed no variation in ultrasonic signal with changes in polarization direction. These polarization effects are attributed to the fact that, in fcc crystals, two distinct shear-wave modes (polarization directions <100> and <110>) can be propagated in the <110> crystallographic direction, whereas only one mode can be generated in the other principle directions. These two <110> shear waves have significantly different sound velocities in stainless steel (by approximately a factor of two) and thus different wave lengths and attenuation properties for any given frequency. For shear waves traveling through a grain in the <110> direction, the attenuation is dependent on the polarization direction. Thus, for specimens with a preferred crystallographic orientation, attenuation may vary with polarization for certain wave-propagation directions, as observed in the specimen described.

This effect may be used to help establish the source of an ultrasonic reflection in an inspection, if the polarization direction of the shear wave can be altered. Similarly, the penetration of a wave may be increased by "tuning" the wave polarization for the particular weld crystallography encountered.

CONCLUSIONS

Differences in microstructure between weld metal and base metal in welded stainless steel components affect the behavior of ultrasonic waves. These differences cause variation in sound velocity and attenuation, giving rise to spurious reflections and reducing the effectiveness of shear-wave inspections. Some improvement is possible by proper choice of frequency, polarization, and type of sound waves. The effects could also be used for material characterization such as preferred crystal orientation, grain-size determination and others, but more effort in this direction is needed.

ACKNOWLEDGMENTS

We wish to thank N. F. Fiore, Notre Dame University, for supplying some weld samples and several of the micrographs.

REFERENCES

1. J. P. Pelseneer and G. Louis, Ultrasonic Testing of Austenitic Steel Casting and Welds, Brit. J. NDT, 16, 107 (July 1974).

2. E. T. Hughes, The Longitudinal Mode for Angle Beam UT of Coarse Grain Austenitic Materials and Welds, ASNT 33rd Nat. Fall Conf., Chicago, Illinois, U.S.A., Oct. 1-5, 1973.

3. D. Beecham, Ultrasonic Scatter in Metals -- Its Properties and Its Application to Grain Size Determination, Ultrasonics 4, 67 (1966).

4. S. Matsumoto and K. Kimura, The Relation between Grain Size and Ultrasonic Attenuation Coefficient in Austenitic Stainless Steel and Iron, Trans. Nat. Res. Inst. for Metals, 14, (4), 21, (1972).

5. R. Hill, The Elastic Behavior of a Crystalline Aggregate, Proc. Phys. Soc. 65, 349, (1952).

6. M. C. Mangalick and N. F. Fiore, Orientation Dependence of Dislocation Damping and Elastic Constants in Fe-18Cr-Ni Single Crystals, Trans. Met. Soc. AIME 242, 2363, (1968).

7. O. R. Gericke, Ultrasonic Spectroscopy, in Research Techniques in Nondestructive Testing, S. R. Sharpe, ed., 1970, 31, Academic Press, New York.

8. A. F. Brown, Materials Testing by Ultrasonic Spectroscopy, Ultrasonics 11, 202, (1973).

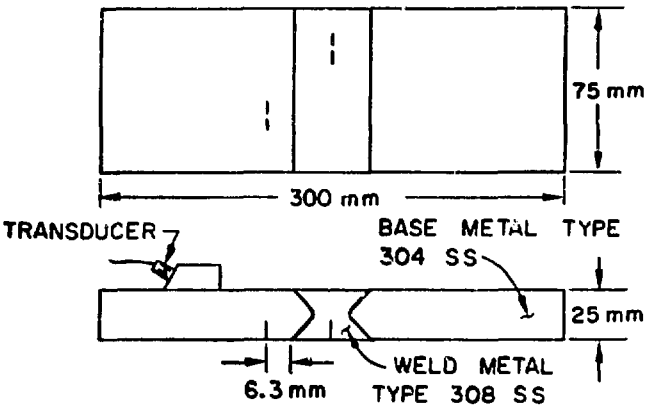

Fig. 1. Flat Type 304 Stainless Steel Specimens Showing Weld Metal and Notches. Neg. No. MSD-62966.

Fig. 2. Plate 2A Base Metal. Mag. 250X.
Neg. No. MSD-62970.

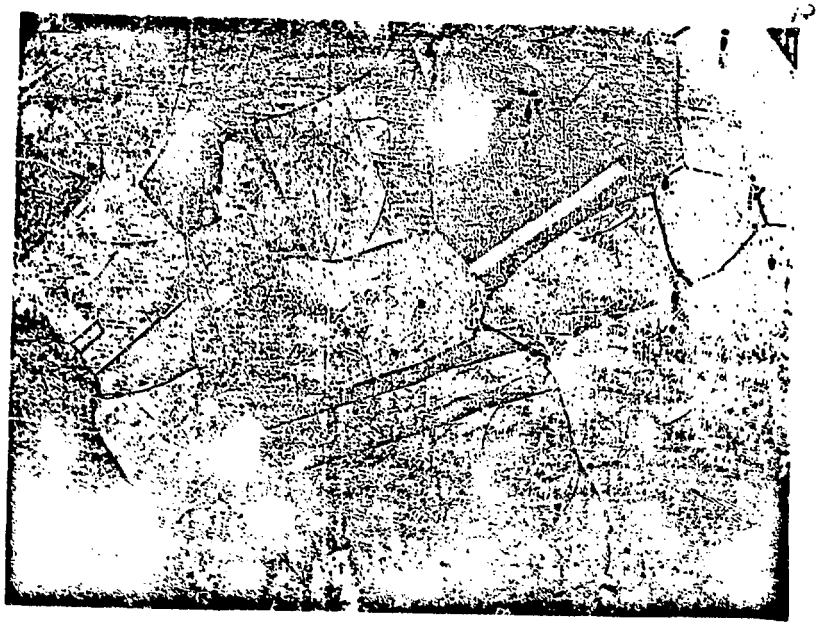

Fig. 3. Plate 4A Base Metal and HAZ.
Mag. 250X. Neg. No. MSD-62971.

Fig. 4. Specimen Half before Welding Showing Macroetching of the Surface. MSD Neg. No. 62232.

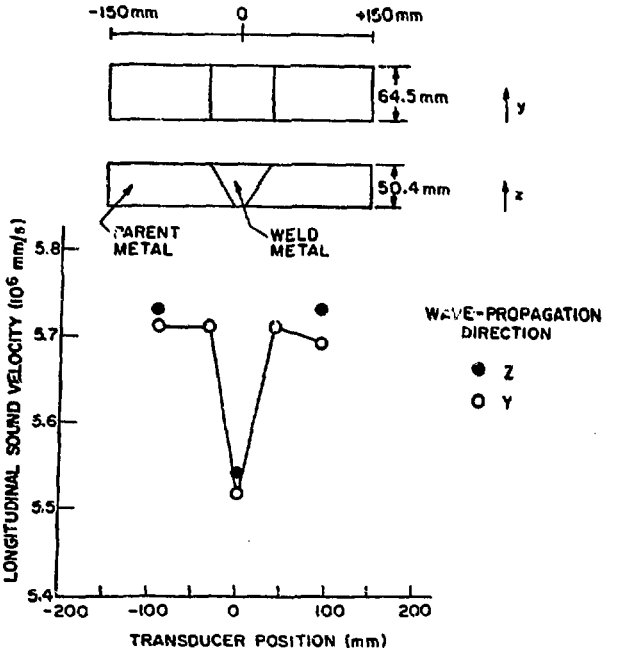

Fig. 5. Variation in Longitudinal Velocity of Sound for 2-in.-thick Welded Austenitic Stainless Steel Plate. Neg. No. MSD-62239.

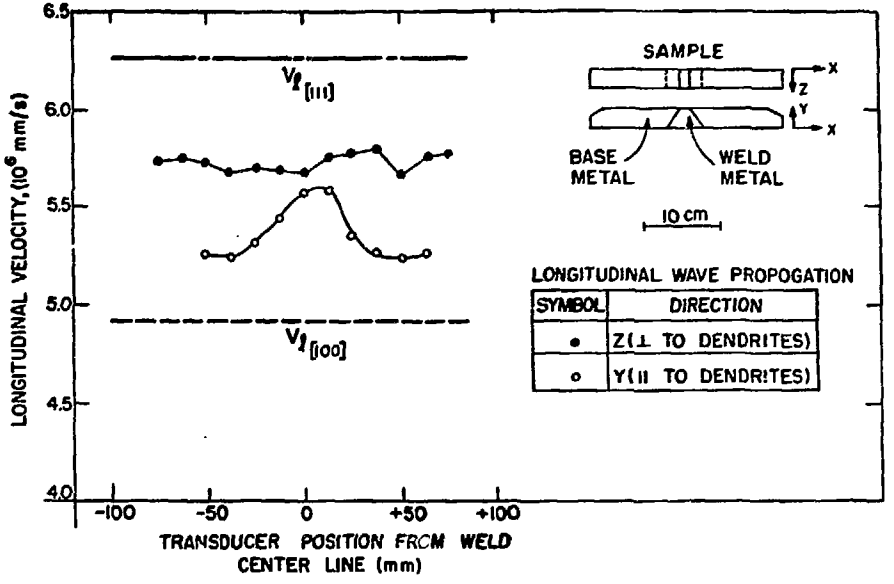

Fig. 6. Longitudinal Velocity of Sound vs Position for Cast Stainless Steel Sample. Neg. No. MSD-

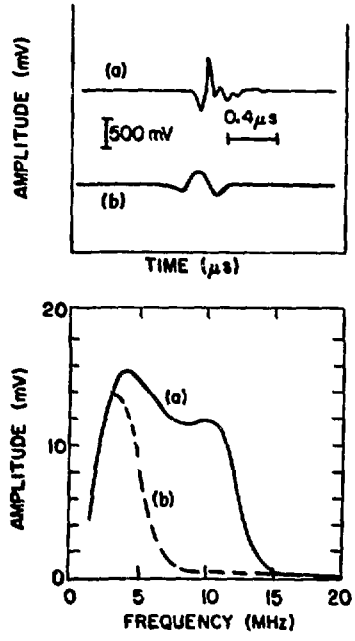

304 S.S.
SAMPLE THICKNESS
2.5 cm
HEAT TREATMENT
(a) ½h AT 954 °C
(b) ½h AT 1121 °C
ACOUSTIC MODE:
LONGITUDINAL

Fig. 7. "A" Scan and Frequency Spectra Obtained Using Longitudinal Waves in Two Type 304 Stainless Steel Samples Heat Treated at Different Temperatures. Neg. No. MSD-62575.

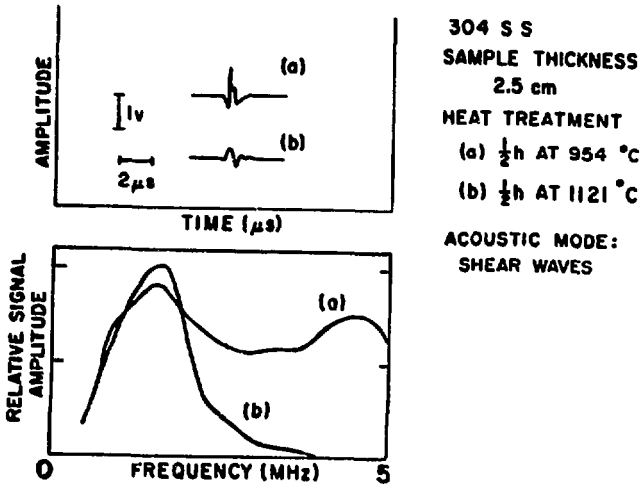

Fig. 8. "A" Scan and Frequency Spectra Obtained Using Shear Waves in Two Type 304 Stainless Steel Samples Heat Treated at Different Temperatures. Neg. No. MSD-62574.

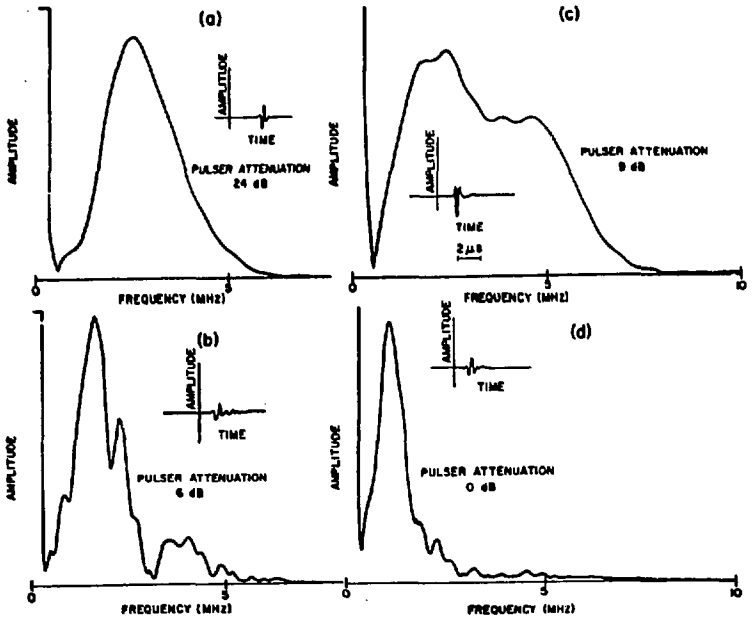

Fig. 9. Frequency Spectra for Austenitic Stainless Steel Welds. (a) Base metal, wave propagation in direction perpendicular to weld-pass direction; (b) through weld metal, wave propagation in direction of weld pass; and (d) through weld metal, in direction of weld pass. The rf "A"-scans for each spectrum are also shown. Neg. No. MSD-62237.

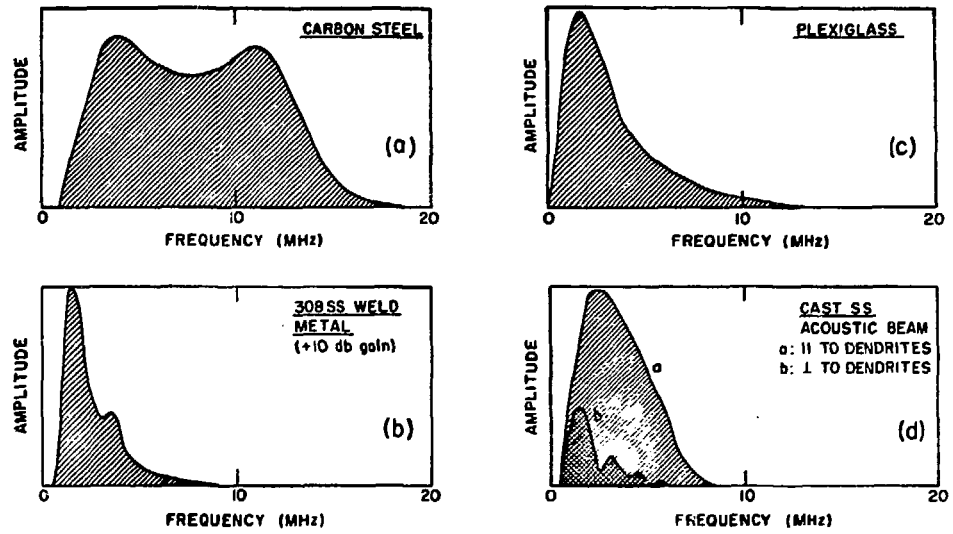

Fig. 10. Ultrasonic-frequency Spectrum of Carbon Steel, Cast Stainless Steel (Base Metal and Weld Metal), and Plexiglass, obtained with longitudinal waves. Neg. No. MSD

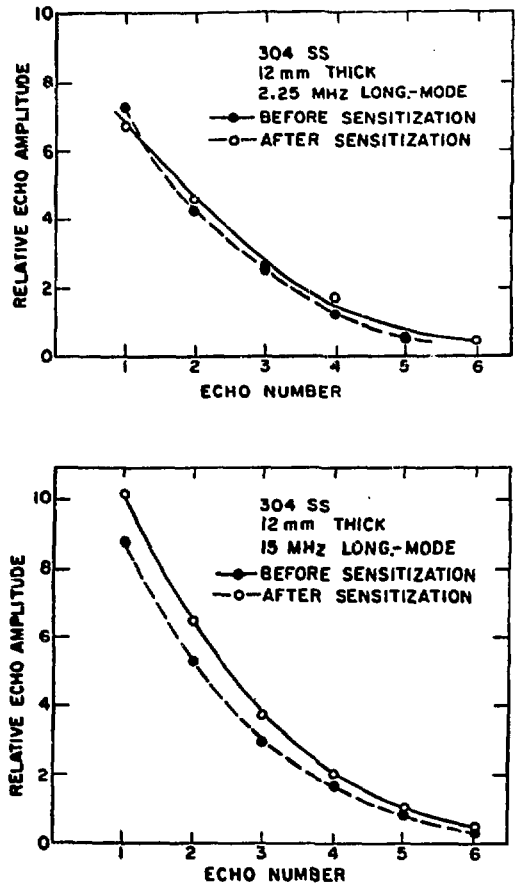

Fig. 11. Echo Amplitudes before and after Sensitization of Type 304 Stainless Steel Specimens for 2.25- and 15-MHz Longitudinal-mode Transducer. Neg. No. MSD-62577.

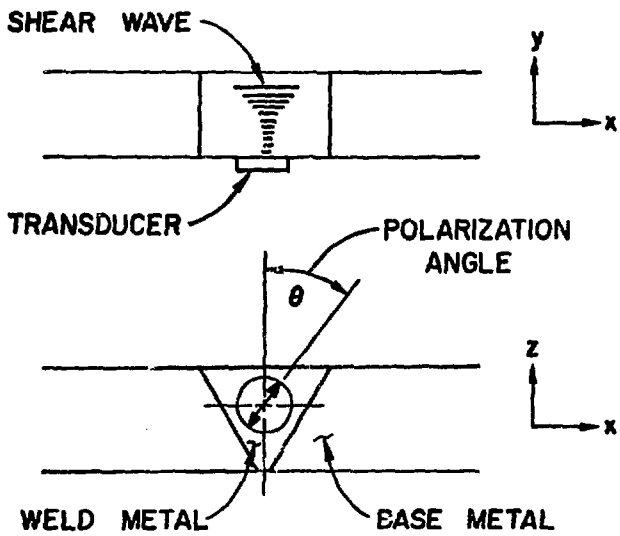

Fig. 12. Stainless Steel Specimen, 300 x 25 x 25 mm, Used for Studies of Shear-wave Polarization Effects in Stainless Steel Weld Metal. Neg. No. MSD-62965.

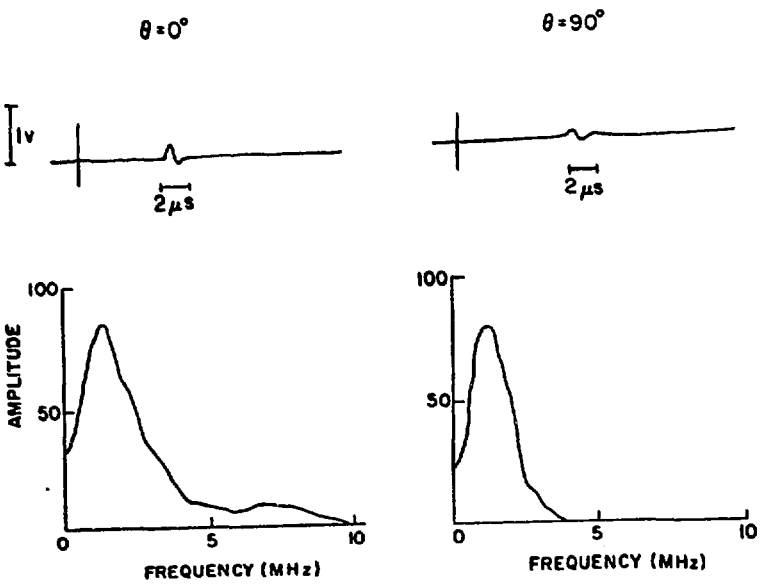

Fig. 13. Radio-frequency "A" Scan and Frequency Spectra of Shear Waves Propagated through the Weld as Shown in Fig. 1.6. Two wave polarization angles are shown, $\theta = 0$ and $\theta = 90°$. Neg. No. MSD-62967.